

# A methodology for the optimization of PCD compact core drilling in basalt rock

R. F. Hamade · F. Pusavec · S. P. Manthri ·  
O. W. Dillon Jr. · I. S. Jawahir

Received: 7 July 2010 / Accepted: 10 October 2011 / Published online: 1 November 2011  
© Springer-Verlag London Limited 2011

**Abstract** This work presents an optimization technique using genetic algorithm for efficient core drilling in basalt rock. Optimization of the compact core-drilling problem is based on maximizing a desirability function which accounts for (a) maximizing the drilling feed while minimizing tool-wear progression, (b) minimizing the thrust force and torque (power), and (c) satisfying realistic constraints related to process parameters. The resulting set of optimized cutting parameters is sought in order to make the tool last longer while effectively drilling with high productivity. A room temperature model to relate the experimental data on changing drill forces and torques required by the progressive tool wear, and developed in a previous paper, is used in this study.

**Keywords** Mars · Basalt · PCD · Drilling · Optimization · Genetic algorithm · Torque · Thrust force · Wear

## 1 Introduction

In the likelihood of robotic exploration on Mars to look for scientific clues, drilling in the Martian crust will likely

involve contact with many types of rock. Basalt, a commonly occurring rock in the earth's crust is also known to be present in abundance on the Mars [1] surface. Other types of softer rock such as limestone are also present there, but being softer, they do not pose such a challenging task as drilling in the hard and abrasive basalt. In addition to its abrasive properties, basalt's hardness and strength make it a formidable material for causing drill wear and with the subsequent rise in thrust force and torque, is a major reliability concern. These challenges are, in a technical sense, similar to those faced when drilling in glass fiber composites [2] or ceramic matrix composites [3] where abrasive and hard constituents are major tool durability concerns.

On Mars, one of the major issues affecting the drilling reliability and longevity involve acceptable levels of thrust force and torque. The latter is the major contributor to power required to carry the actual cutting while a minimum vertical force on the tool is required for efficient drilling action to commence. Glowka [4, 5] developed algorithms for a computer code (PDCWEAR) that predicts the performance and wear of polycrystalline diamond (PCD) drill bits. Recently [6], Tulu et al. developed a cutter-rock model to account for the influence of several factors including bit design and drilling parameters. In anticipation for the exploration of Mars, studies on drilling in basalt rock formations have in recent years become increasingly relevant and significant. Specific to compact core drilling in basalt, Zacny and Cooper [7] utilized a conventional, core rotary drilling approach using a polycrystalline diamond (PCD) drill bit. Hamade et al. [8–10] utilized a similar setup to study tool wear and the corresponding cutting forces. Two modes of gradual tool wear were monitored: flank wear (VB) and cutting edge radius (CER) wear.

Once mathematical equations have been determined, such as what was done in Hamade et al. [10], which

---

R. F. Hamade (✉)  
Department of Mechanical Engineering,  
American University of Beirut (AUB),  
Beirut, Lebanon  
e-mail: rh13@aub.edu.lb

F. Pusavec  
Faculty of Mechanical Engineering, University of Ljubljana,  
Askerceva 6,  
1000 Ljubljana, Slovenia

S. P. Manthri · O. W. Dillon Jr. · I. S. Jawahir  
Department of Mechanical Engineering,  
Institute for Sustainable Manufacturing, University of Kentucky,  
Lexington, KY 40506, USA

describe the dependent cutting variables in terms of independent ones, an optimization technique is used to identify a set of input parameters that result in an “optimum” performance. For example, optimization of rock cutting operations of both large diameter (e.g., [11, 12]) and compact scale (e.g., [13, 14]) operations have long been attempted with the aim of improving tool life, and consequently, penetration depth.

Genetic algorithms (GA) [15] are an example of nature-based evolutionary algorithmic techniques that have gained considerable attention in the area of optimization. In metal cutting, classical solutions of the typical optimization problem involve maximizing material removal rate (MRR) subject to constraints on such parameters as speed, feed, and tool life (e.g., [16]). GA techniques have gained popularity in many applications including those geared towards solving machining-related multi-objective optimization problems [17–19]. Wang and Jawahir [20] developed a comprehensive optimization criterion for turning operations considering the effect of progressive tool wear and using genetic algorithms to select the best cutting conditions and tool geometry. In rock drilling, optimization work by Clayton et al. [21] aimed to “achieve an optimum match in drilling efficiency and bit life” by customizing the model for “optimizing cutting efficiency and durability according to specific rock properties and drilling parameters.” The authors are not aware of any published work in the rock cutting literature that addresses the optimization of tool life in compact core-drilling applications by minimizing tool wear in a fashion similar to the work presented in this paper. GA is used to solve the optimization problem with emphasis on maximizing tool life in basalt rock given the overriding sustainability requirement. Specifically, we optimize, using GA, the drill-wear process for maximum feed while minimizing the thrust force and torque (power) and minimizing tool wear, using previously developed [10] models for tool wear and cutting forces.

## 2 Methodology

Geological models to predict the mechanics and performance of drills in deep well drilling as a function of rock geology do exist and their outputs are in common use today when determining the quality of the drilled bore. The parameters that contribute to force generation and tool wear from these rather complex models were found to include unconfined rock strength (UCS). However, predicting performance of bore drilling in complex geological formations can be very demanding and involves many parameters (see for example, [22]) and with many factors influencing bit wear [23]. In controlled, smaller-scale

drilling experiments, it is hoped that many potential complications resulting from rock peculiarities—such as material inhomogeneity, powder generation, and catastrophic failure (cracking)—may be avoided. For such experiments, process parameters (treated as input variables) may be varied and the cutting forces and tool wear (treated as output variables) are monitored. Traditionally, several modes of tool wear have been studied; prime among them are flank wear, an increase in the cutting edge radius, and crater wear.

The compact drilling methodology program may be summarized as follows:

1. Develop a validated model of progressive tool wear in terms of the many process variables including: rock strength, tool geometry, and drilling parameters (spindle speed and drill tool feed). Such a model was recently developed by the authors [10] which consisted of:
  - a. Suitable core-drill configuration and inserts: the configuration chosen in this work contains four PCD inserts (see the section 3 for more details).
  - b. Test matrix to account for variables such as rock strength (two different UCS rocks), process variables (tool feed, rpm), and tool geometry (rake angle).
  - c. Monitoring and measuring of gradual tool wear: VB and CER wear under different rocks strength and drilling conditions.
  - d. Deriving equations to model gradual tool wear as a function of the variables (1.b.)
2. For the same setup, develop a validated model of the generated thrust force and torque during core drilling which relate these forces to the process variables as well as progressive tool wear captured in step 1 above. This involves:
  - a. Monitor and measure the generated thrust force and torque as function of the variables (1.b).
  - b. Derive equations to model thrust force and torque as function of those variables.

Although such models were developed in Ref. [10], in this paper the authors advance a mathematical model which, unlike the previous equations, does not account explicitly for tool-wear effect of wear on the cutting forces. These new forms are more suitable for optimization purposes.

3. Develop an optimization routine to obtain an optimized set of the process parameters (1.b) that results in the desired objective(s) (e.g., maximum volume removed) while meeting certain constraints on operational parameters.

### 3 Experimental work

The compact core-drill configuration utilizes four PCD compact inserts (grade—CTH, supplied by Diamond Abrasives Corp. (now Element Six Inc.), New York, USA). The PCD compact inserts are manufactured by sintering selected synthetic diamond particles at very high temperature and pressure in a solvent/catalyst metal. The resulting thickness of the diamond layer is approximately 0.5 mm, with average diamond particle size of 25 μm. The PCD is brazed on a substrate of tungsten carbide. Figure 1 is a schematic illustration of the individual rectangular (wedge angle=90°) tool insert with dimensions of 6.0×3.5×1.6 mm. The two internal inserts generate the inner diameter of the bore (of 25 mm) while the outer two inserts prescribe the outer bore diameter (of 38 mm). In the experimental setup, the PCD inserts are oriented at negative rake angles (supported with removable wedges).

In order to simulate the in situ conditions on Mars, all drilling was performed dry. The drilling process variables studied are (1) tool feed (*f*) and (2) spindle speed (rpm). Since the width of cut is constant for the core-drilling configuration (equal to the insert width of 3.5 mm), it is omitted from further consideration. Four levels of tool feed, *f*, (0.01, 0.025, 0.04, and 0.05 mm/rev) are considered in the study, and four levels of spindle speed (60, 100, 140, and 180 rpm) are used in the experiments. Note that tool feed (or simply feed; *f* (mm/rev)) in the drilling literature is referred to as the depth of cut which represents the distance (in mm) the tool travels per spindle revolution. In this type of process, feed is the uncut chip thickness (*h*) which represents the actual chip thickness and is defined as the feed per revolution per cutter. Each set of two PCD inserts cut different portions of the hole (inside or outside). Dividing feed by the number of teeth (2),  $h = f/2$ , yields the *h* value (in mm). Given the hard and abrasive properties of basalt, linear cutting speeds in all the experiments in this

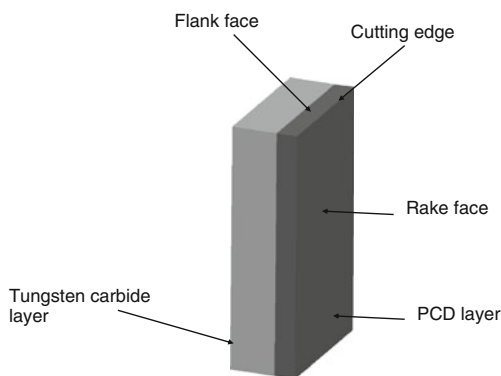


**Fig. 1** Schematic illustrating a cutting PCD insert. Features highlighted include the flank face where VB takes place and the cutting edge where rounding causes bluntness

work are relatively small (e.g., 60 and 180 rpm would result in maximum cutting speeds of 7.2 and 21.5 m/min, respectively).

Also studied is the tool’s rake orientation with respect to the rock (rake angle) where four levels of negative rake angle,  $\alpha$ , ( $-5^\circ$ ,  $-10^\circ$ ,  $-15^\circ$ , and  $-25^\circ$ ) were evaluated. The experimental plans for rake angle and cutting conditions variations to be used in the optimization program are chosen using the Taguchi design of experiments principles (L16 orthogonal array). The Taguchi method reduces the number of needed experiments from 64 in the full factorial plan to 16.

In addition to the drilling process parameters and rake angle, the effect of the rock’s UCS was also studied. Therefore, for all 16 experiments, VB measurements were made at total drilling depths of 15, 30, 45, 60, and 75 mm in two different formations of Duluth basalt rock: one designated as “soft” and the other “hard” with estimated UCS values of 240 and 350 MPa, respectively. See Ref. [10] for details on insert wear and force and torque measurements.

### 4 Modeling drilling force and torque

Core-drilling experiments in basalt reveal that the initial force and torque values that correspond to the sharp cutting edge gradually increases. The initial value is a function of rock strength as well as the process parameters. The gradual increase in the force and torque value is proportional to insert wear (e.g., [4, 24]). Also observed is that force and torque rate increase is smaller in soft basalt than in hard basalt. Taking the above into consideration, power forms are used [10] to mathematically describe the thrust force (*F*) and torque (*T*)

$$F = F_0 \times \{ \lambda_F^{\alpha 1} \times UCS^{\beta 1} \} \times \{ f^{\chi 1} \times rpm^{\delta 1} \times (1 - \sin \alpha)^{\varepsilon 1} \} \times hole\_depth^{\gamma 1} \tag{1}$$

$$T = T_0 \times \{ \lambda_T^{\alpha 2} \times UCS^{\beta 2} \} \times \{ f^{\chi 2} \times rpm^{\delta 2} \times (1 - \sin \alpha)^{\varepsilon 2} \} \times hole\_depth^{\gamma 2} \tag{2}$$

where the variables have been defined above, except for  $\lambda_F$ ,  $\lambda_T$  and hole\_depth which are described next. Also,  $\alpha 1$ ,  $\beta 1$ ,  $\chi 1$ ,  $\delta 1$ ,  $\varepsilon 1$ , and  $\gamma 1$  and  $\alpha 2$ ,  $\beta 2$ ,  $\chi 2$ ,  $\delta 2$ ,  $\varepsilon 2$ , and  $\gamma 2$  are power coefficients the values for which are determined via fitting of experimental force and torque data to the forms in Eqs. 1 and 2, respectively.

The power forms in Eqs. 1 and 2 are of the same form as the generalized Taylor’s classical 1907 tool-life law and are quite successful in both metal cutting (see for example, [25] and rock cutting [4]). The variables  $\lambda_F$  and  $\lambda_T$  are needed to account for the rock samples being in the “virgin” or previously “cut” state since the experiments revealed differences due to the sample preparation. Cutting the rocks to a size compatible with mounting in our experimental setup appears to have had an effect on the required drilling  $T$ . Accounting for this effect was accomplished mathematically via the parameters  $\lambda_F$  and  $\lambda_T$  whose values are

$$\lambda_F = \lambda_T = 1 \quad \text{if virgin, “uncut” specimen were used}$$

$$\lambda_F \approx 1, \lambda_T > 1 \quad \text{if thin, previously “cut” specimen were; used}$$

In the second bracket of Eqs. 1 and 2, the expression  $(1 - \sin \alpha)$  has been previously used in metal cutting literature [26] in lieu of other angle-containing expressions since it produces a positive value even when  $\alpha$  or  $\sin \alpha$  are negative. The variable *hole\_depth* represents the distance (in mm) from the hole’s top surface to the tip of the insert’s cutting edge. This variable is included in order to determine whether the position of the cutting tip with respect to the hole’s top has a significant effect on the measured forces.

Note that Eqs. 1 and 2, unlike the models reported in Ref. [10], do not account explicitly for tool-wear causing changes in the forces and torques during cutting. Therefore in Eqs. 1 and 2, the values of the power coefficients will be different than those reported previously [10]. However, the form of Eqs. 1 and 2 is more useful for the optimization purposes such as those sought in this paper.

Utilizing multiple regression analysis (using the nonlinear least squares procedure in MATLAB), the values for the power coefficients  $\alpha_1, \beta_1, \chi, \delta, \varepsilon,$  and  $\gamma$  are determined via fitting the thrust force and torque data collected for all experiments are shown in Table 1. Also shown is the coefficients’ statistical significance as indicated by their respective  $p$  values. The values of “Prob>F”<0.05 indicate that a certain model parameter is significant while values of >0.10 indicate that it is not. The fit also resulted in estimated values of the coefficient of  $\lambda_T$  to be equal to 1.58 and 1.99 for the “soft” and “hard” rocks, respectively, with the values for  $\lambda_F$  to be practically unity (implying no effect of preparation effects on thrust force).

### 5 Modeling insert wear

In this section, a brief summary of the mathematical equations reported in Ref. [10] and based on observations

of worn tool profiles following drilling experiments are presented.

#### 5.1 Flank wear

In the earlier experiments, VB wear was measured after boring holes that are 15 mm deep and was found to be steady and linear with hole depth after an initial (and very rapid break-in period). The behavior was described in Ref. [10] by

$$VB = VB_i + VB_{Wear\_Rate} \times drilled\_depth \tag{3}$$

where  $VB_i$  and  $VB_{Wear\_Rate}$  represent the initial flank wear and the rate of flank wear growth, respectively. In Eq. 3, drilled-depth represents the total distance (in mm) drilled by the insert. Parameters  $VB_i$  and  $VB_{Wear\_Rate}$  were described in terms of UCS, feed ( $f$ ), spindle speed (rpm), and rake angle ( $\alpha$ ) by the following two equations:

$$VB_i = VB_{i0} \times UCS^{a_1} \times f^{b_1} \times rpm^{c_1} \times (1 - \sin \alpha)^{d_1} \tag{4}$$

$$VB_{Wear\_Rate} = VB_{Wear\_Rate_0} \times UCS^{a_2} \times f^{b_2} \times rpm^{c_2} \times (1 - \sin \alpha)^{d_2} \tag{5}$$

In the equations, the parameters are as defined above while  $a_1, b_1, c_1,$  and  $d_1$  and  $a_2, b_2, c_2,$  and  $d_2$  are power coefficients the values for which are determined via fitting of experimental VB wear data to the forms in Eqs. 4 and 5, respectively. While  $VB_i$  represents the break-in stage of

**Table 1** Values of exponents in Eqs. 1 and 2 for thrust force ( $F$ , N) and Torque ( $T$ , N m) and their statistical significance

Variable	Coefficient/exponent	Value	$p$ value
<b>Thrust force (<math>F</math> (N))</b>			
	$F_0$	0.016111	
$\lambda$	$\alpha_1$	0.101599	0.8077
UCS	$\beta_1$	1.856095	<0.0001
Feed	$\chi_1$	0.263652	<0.0001
rpm	$\delta_1$	0.039254	0.6145
1-sin $\alpha$	$\varepsilon_1$	1.606934	<0.0001
Hole_depth	$\eta_1$	0.044042	0.216
<b>Torque (<math>T</math> (N m))</b>			
	$T_0$	0.0018154	
$\lambda$	$\alpha_2$	2.0499854	<0.0001
UCS	$\beta_2$	1.5777541	<0.0001
Feed	$\chi_2$	0.4212394	<0.0001
rpm	$\delta_2$	-0.140501	0.0094
1-sin $\alpha$	$\varepsilon_2$	-0.628601	0.0093
Hole_depth	$\eta_2$	0.0301592	0.2192

wear,  $VB_{Wear\_Rate}$  represents the near constant wear rate during the steady-state stage of the wear growth.

### 5.2 Cutting edge radius wear

Having experimentally determined the initial values as well as the progression rate of the wear in the insert’s cutting edge radius wear, the wear behavior was [10] described mathematically by

$$CER = CER_i + CER_{Wear\_Rate} \times drilled\_depth \tag{6}$$

in a fashion similar to that for VB. While the average initial value of the  $CER_i$  was measured to be  $CER_i = 6.5 \mu m$ , CER wear rate is described by

$$CER_{Wear\_Rate} = CER_{Wear\_Rate_0} \times UCS^{a_3} \times f^{b_3} \times rpm^{c_3} \times (1 - \sin \alpha)^{d_3} \tag{7}$$

where  $a_3, b_3, c_3,$  and  $d_3$  are power coefficients determined from fitting experimental cutting edge radius data to the forms in Eq. 7.

### 5.3 Insert-wear results

The nonlinear least squares procedure in MATLAB was used to fit the experimentally determined values of initial flank wear and wear rate data to Eqs. 4 and 5. The resulting exponent values and statistical significance (as indicated by their respective  $p$  values) are presented in Table 2. The table also lists the values for the CER wear exponents in Eq. 7 along with their statistical significance. The results indicate strong statistical significance influence of the tool’s feed as well as of rake angle on the wear rate of the CER. For example, the near unity values for  $a_2$  (0.872;  $p=0.0176$ , statistically very significant) and  $a_3$  (1.062;  $p=0.001$ , statistically very significant) suggest that VB and CER wear rates increase almost linearly with rock strength. This is consistent with other reported findings in rock cutting [27].

**Table 2** Values and their statistical significance of exponents in Eqs. 4, 5, and 7 [10]

Equation 4					
Log $VB_{i0}$	$a_1$	$b_1$	$c_1$	$d_1$	
-1.8579	0.3401	-0.0555	-0.0967	-0.6238	
$p$ value	0.0125	0.187	0.128	0.0218	
Equation 5					
Log $VB_{Wear\_Rate_0}$	$a_2$	$b_2$	$c_2$	$d_2$	
-4.5371	0.8718	-0.2716	-0.4855	-1.6914	
$p$ value	0.0176	0.0216	0.0072	0.0219	
Equation 7					
Log $CER_{Wear\_Rate_0}$	$a_3$	$b_3$	$c_3$	$d_3$	
-3.3306	1.0623	0.1370	-0.0088	2.2330	
$p$ value	0.001	0.073	0.937	0.001	

## 6 Optimization of core-drilling parameters

In the following, we utilize the above equations describing tool wear and force in order to obtain the parameters for optimum behavior of the core drilling process. Therefore, the latent benefit of models, in equation form, is that they may be used to establish the thrust force (or torque) as well as rock strength, process parameters, and rake angle, that will be a more sustainable core-drilling process. One may be able to solve the above equations to predict both forms of tool wear (VB and CER) in the PCD inserts. However, one more important contribution is their usage as an input to the overall optimization process, to enhance overall drilling efficiency. This could be quite useful in achieving sustainable remote drilling operations such as on Mars expeditions.

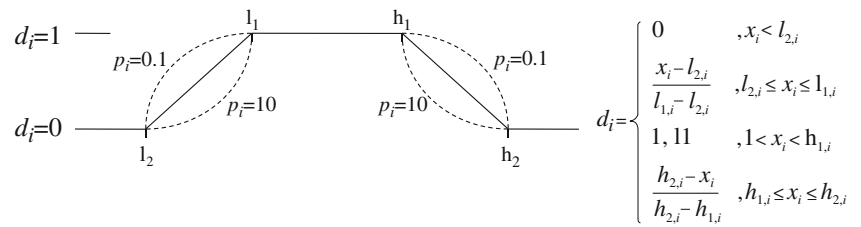
Optimization of the machining process comprises the determination of an optimal set of the machining conditions that satisfy an objective with several constraints. In this work, the machinability criterion used is maximizing material removal rate, while assuring low cutting force, torque and tool wear are adopted as the objectives. Rotational speed ( $rpm$ ), tool feed ( $f$ ), and rake angle ( $\alpha$ ) are used as system variables. The optimization technique used in this work is the GA [15].

### 6.1 Optimization objectives

In practice, there is always more than one process objective and/or constraint. To find the optimal cutting parameters for the cutting process, an objective function has to be defined so that it satisfies all the process objectives and constraints. This objective function consists of several sub-objective functions corresponding to each of the objectives/constraints. How good a set of calculated parameters are suited to each of the objectives/constraints has to be independently evaluated. However, in order to obtain a solution set suitable for the whole problem, the goals of optimization



**Fig. 2** Individual desirability function representation



are usually combined into an overall desirability function  $D(x)$ . The optimization technique will then, based on this desirability function, determine the optimal solution for the specific process.

The multi-objective optimization problem of core drilling in Martian rock treats the cutting parameters feed, rpm, tool rake angle, hole depth, and rock strength as input parameters with the responses being thrust force, torque, and tool-wear VB and CER. These objectives are to: (1) maximize penetration rate (feed) for high productivity while (2) minimizing the cutting force/torque, and (3) minimizing tool-wear VB and CER. The first objective guarantees that the process is energy efficient given that higher feeds translate into lower specific cutting energy (coefficients). Furthermore, maximize tool penetration, feed, resulting in high MRR. (Although an alternate and potentially feasible objective is to maximize (tool wear/MRR), it was not investigated in this work). The second objective is concerned with practical limitations on available power on the robotic arm. The third objective has the natural outcome of enhancing the sustainability of the difficult to replace cutting tools by maximizing their life for enhanced sustainability. This objective also addresses energy preservation since sharper tools contribute to lower specific cutting energy (defined as the work needed to remove a given volume of the rock according to [14]). Since smaller forces generally imply lower stresses, the optimum solution resulting from these combined objectives also implies less probability of catastrophic tool breakage (as compared to just progressive tool wear).

To satisfy these apparently conflicting sub-objectives of the optimization, the so-called “overall desirability” function is utilized. The overall desirability function has to account for all sub-objectives and constraints and, therefore, has to be composed of the individual desirability functions so that each one of the posed sub-objectives/constraints is satisfied. In this work, the overall desirability function consists of 8 individual ones (three of them defining cutting parameter ranges, two for cutting thrust force and torque, two for tool wear, and one for material removal rate).

6.2 Individual desirability function— $d_i$

The individual constraint desirability function corresponds to the equation shown in Fig. 2. For simultaneous

optimization, each response must have desirability function arranged to satisfy the individual constraints. This can be achieved with defining the limitation levels of equation in Fig. 2 ( $l_1, l_2, h_1,$  and  $h_2$ ). The cutting parameters have to be equal to experimental design space and therefore they have to be in the range used in the experiments ( $l_2=l_1$ =low value of the parameter and  $h_1=h_2$ =high value of the parameter). The tool wear has to be as low as possible (VB— $l_2=0$  and  $l_1=h_1=h_2$ =limitation of tool life=0.15 mm; CER— $l_2=0$  and  $l_1=h_1=h_2$ =limitation of tool life=20  $\mu$ m). The cutting thrust force and torque have to be as low as possible ( $l_2=0$  and  $l_1=h_1=h_2$ =worst case). The last goal of the optimization is to increase the productivity, in this case through higher penetration rate (feed rate,  $f$  ( $l_2=l_1=h_1=0, h_2$ =best of all experiments)). In all the cases, the relations were taken as linear therefore  $p_i=1$ , and equally weighted [28].

The desirable values for the desirable function range from 0 (least desirable) to 1 (most desirable). If any of the responses or parameters fall outside their desirability range, the function become 0 and will later lead into zero overall desirability function. These ranges and the associated objectives associated with each parameter are tabulated in Table 3.

The constraints placed on feed rate, cutting speed, and rake angle are provided by the core drill supplier so as not to cause catastrophic PCD insert failures. The rest of the constraints are bound by the ranges utilized in the experiments. This implies that this work does not support extrapolations of values outside of these ranges.

**Table 3** Optimization objectives and constraints

	Constraint	Objective
Feed ( $f$ (mm/rev))	$0.01 \leq \text{feed} \leq 0.05$	In range (maximize)
Spindle speed (rpm)	$60 \leq \text{speed} \leq 180$	In range
Rake angle ( $\alpha$ )	$-5^\circ \leq \alpha \leq -25^\circ$	In range
Hole_depth	Depth=3 mm	Fixed
$\lambda$	$1 \leq \lambda \leq 1.99$	In range
UCS (MPa)	$240 \leq \text{UCS} \leq 350$	In range
Thrust force ( $F$ (N))	$0 \leq F \leq 1,000$	In range (minimize)
Torque ( $T$ (N m))	$0 \leq T \leq 5$	In range (minimize)
Flank wear (VB (mm))	$0 \leq \text{VB} \leq 0.15$	In range (minimize)
Edge wear (CER ( $\mu$ m))	$0 \leq \text{CER} \leq 20$	In range (minimize)

### 6.3 Overall desirability function

In this work, the response surface method [28] is used to model the process. Consequently, a desirability function based on the multiple response method is used in the modified form in the following

$$D(x) = \left( \prod_{i=1}^n ((d_i)^{p_i})^{w_i} \right) \frac{1}{\sum_{i=1}^n w_i} \quad (8)$$

where  $d_i$  are individual constraint desirability functions,  $p_i$  are nonlinear responses of individual constraints,  $n$  is the number of constraints included in the optimization procedure and  $w_i$  are the weights (weighted equally,  $w_i=1$ ) belonging to each of the constraints.

It reflects the desirable ranges for each constrain  $d_i$ . These constraints produce the system that can be solved via the use of an overall desirability function  $D(x)$ . With defined evaluation of the process through desirability function,  $D(x)$ , the optimization can proceed. The best solution represents the case where the desirability function has the highest value. To find this combination of parameters, the Genetic Algorithms evolutionary searching methodology is used. While a custom script was written for the modeling and desirability function routines, the GA tool-box of MATABL was used for the optimization procedure. A flow diagram illustrating the optimization procedure is outlined in Fig. 3.

### 6.4 GA procedure

As described above, with the combination of input parameters, the desired best responses can be defined. Optimization runs for 100 generations, each having a population size of 1,000 individuals, of which two individuals are guaranteed to survive are utilized. The mutation probability decreases linearly with subsequent generations,  $p_{mut}=1-i_{gen}/100$ , and the crossover probability was 0.8. The initial ranges of parameters were randomly generated on the following ranges ( $f$ , rpm,  $\alpha$ ,  $\lambda$ , UCS, hole\_depth)=(0.01:0.05, 60:180, -25:-5, 1:1.99, 240:350, 3.0:3.0).

### 6.5 Optimization results

As described above with the compromising combination of input parameters, the desired best responses are defined as the one with largest value of  $D(x)$ . The results obtained by executing this optimization procedure are represented in Fig. 4. Presented in this figure are relations of process input parameters to the desirability function as an estimator of overall process performance. This figure presents the selection of optimal cutting parameters based on the

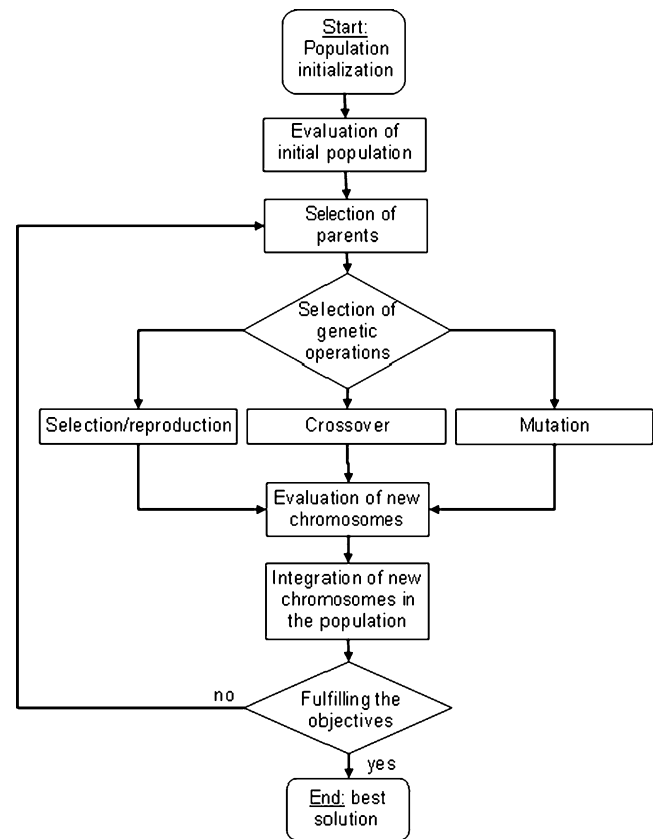


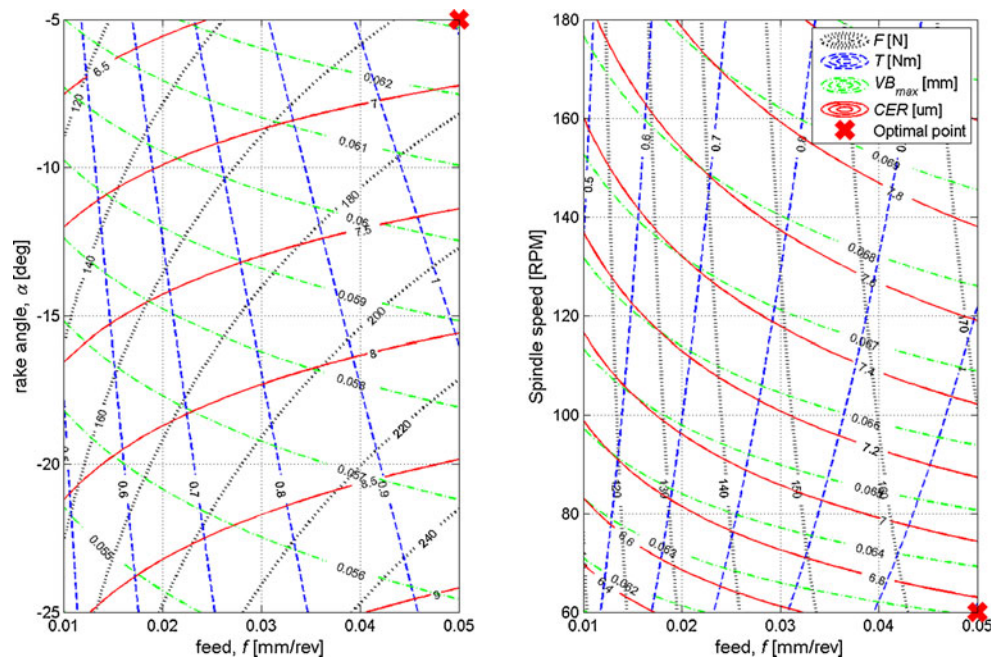
**Fig. 3** A flow diagram illustrating the optimization procedure using genetic algorithm

evaluation of desirability that has to be maximized. Shown marked (with an “x” symbol) on both figures is the value of the maximized desirability function.

The optimum parameters were found (Table 4) to be: tool feed=0.05 mm/rev, spindle speed=60 rpm, rake angle,  $\alpha=-5^\circ$ ,  $\lambda=1$  and UCS=240 MPa. Indicated desirability function value was  $D(x)=0.89$ . Based on these results, it can be concluded that optimal cutting conditions are indicated by shifting feed to the maximum of the range used while cutting speed and rake angle are at the minimum limit of the range used in this study. The resulting forces and wear are low. For these conditions and at fixed depth set to 3 mm, the table indicates corresponding values of process outputs: thrust force=165 N, torque=1.08 Nm, tool-wear VB=0.06 mm, and tool-wear CER=6.71 mm. The predicted force of 166 N is much lower than the available thrust force on Mars which is estimated at 1,000 N.

These findings are further presented in Fig. 5 via a graphical representation of the optimum values within the whole range of input parameters and output measures. For clarity, the input parameters occupy the upper half of the figure while the output measures (thrust force, torque, tool flank wear, and tool edge wear) reside in the bottom half.

**Fig. 4** Relations of process input parameters to outputs for defining the overall process optimum performance and process input/output parameters. The same legend applies to both figures



The effect of rock strength on the optimization results was further checked. When UCS was forced to increase from the (optimum) soft rock to a hard UCS of 350 MPa (maximum limit) the code returned the same set of values for the input parameters (feed, rotational speed, and rake angle) as in Table 4. This is due to the fact that the optimum values of the input parameters are already at their extreme (lower or upper) limits in Table 3 and did not change due to the change in UCS. However, as compared with Fig. 5 (UCS=240 MPa), the values of the output measures for UCS=340 MPa have increased to: thrust force=332 N, torque=1.94 Nm, tool-wear VB=0.08 mm, and tool-wear CER=7.09 mm. Therefore, one should refer to the UCS “spoke” in Fig. 5 only as an indication of the desired UCS value to which the code returned the indicated output measures values. For values of UCS other than 240 MPa, the values of the output measures will be different from those shown in the figure as was just illustrated. The finding that drilling in softer rock requires lower forces and causes less wear than in hard rock is both intuitive and in line with previous findings [10].

Based on the above optimization results it can be concluded that with selection of optimum cutting conditions taking into account tight constraints, it is possible to provide sustainable machining performance of Martian basalt rock drilling process.

**Table 4** Optimized cutting parameters which maximize  $D(x)$

$f$ (mm/rev)	Spindle (rpm)	$\alpha$ (deg)	$\lambda$	UCS (MPa)
0.05	60	-5	1	240
$F$ (N)	$T$ (N m)	VB (mm)	CER ( $\mu\text{m}$ )	$D(x)$
166	1.1	0.06	6.71	0.89

### 7 Summary

Combining the two aforementioned models (force data model and the corresponding tool-wear model) has yielded a desirable set of cutting conditions which resulted in an optimized tool feed (for enhanced productivity) while

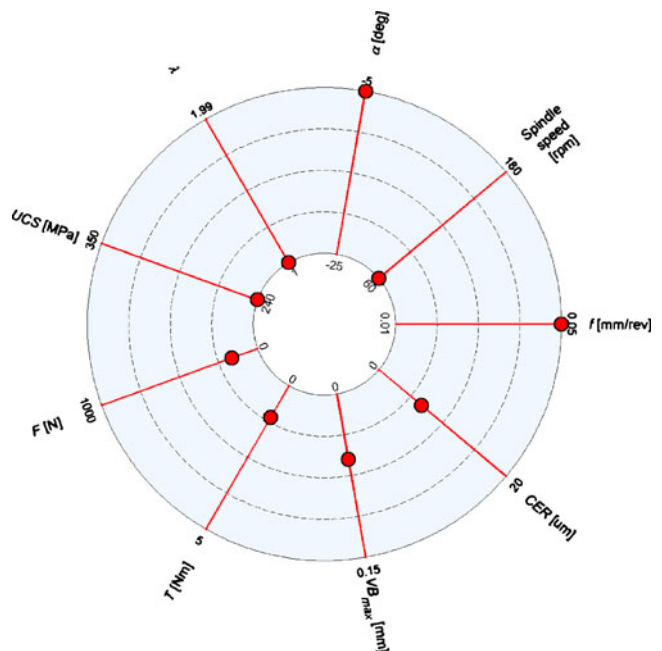


**Fig. 5** Optimum cutting condition representation with respect to the corresponding output measures (thrust force, torque, tool flank wear, tool edge wear, and indirect productivity measure through penetration rate). Optimum is represented with the following input parameters:  $f=0.05$  mm/rev; rpm=60 rpm; and  $\alpha=-5^\circ$



minimizing forces and tool wear. These optimized core drilling parameters insure longer tool life and, thus, enhanced drilling sustainability on Mars and provide guidance to exploration planners. An implicit benefit is that the optimized solution, by the virtue of lowering cutting forces, results in lowering the probability of catastrophic tool failure. This method of obtaining an optimized solution is practical because the models for forces and wear are in equation form. It is worth noting that for this work to be directly applicable to a Mars exploration trip, the temperature effect will also have to be considered. Therefore, future work will involve drilling at the cold temperatures prevalent on this planet. Another issue, which will have to be considered, is chip removal to avoid potential tool clogging.

**Acknowledgements** The financial support of Kentucky Science and Engineering Foundation, KSEF (Emerging Ideas—Materials Science and Advanced Manufacturing grant #KSEF RDE-008) is appreciated. The first author wishes to acknowledge the financial support of the University Research Board (URB) of the American University of Beirut.

## References

- Ferguson RL, Christensen PR, Bell JF III, Golombek MP, Herkenhoff KE, Kieffer HH (2006) Physical properties of the Mars exploration rover landing sites as inferred from mini-TES-derived thermal inertia. *J Geophysical Research* 111:E02S21
- Fernandes M, Cook C (2006) Drilling of carbon composites using a one shot drill bit. Part II: empirical modeling of maximum thrust force. *Int J of Machine Tools and Manufacture* 46(1):76–79
- Lia ZC, Jiaoa Y, Deinesa TW, Peia ZJ, Treadwell C (2005) Rotary ultrasonic machining of ceramic matrix composites: feasibility study and designed experiments. *Int J Mach Tool Manuf* 45:1402–1411
- Glowka DA (1989) Use of single cutter data in the analysis of PDC bit designs: part 1—development of a PDC cutting force model. *J Petrol Tech* 41(8):797–799 (844–849)
- Glowka DA (1989) Use of single-cutter data in the analysis of PDC Bit designs: part 2—development and use of the PDCWEAR computer code. *J Petroleum Technology* 41(8):850–859
- Tulu IB, Heasley KA, Bilgesu I, Sunal O (2008) Modeling rock and drill cutter behavior. In: 42nd U.S. rock mechanics—2nd U. S.–Canada rock mechanics symposium 2008 proceedings, San Francisco, CA, USA, 29 June–2 July 2008
- Zacny KA, Cooper GA (2004) Investigation of diamond-impregnated drill bit wear while drilling under Earth and Mars conditions. *J Geophys Res* 109(E7):E07S10
- Hamade RF, Manthri SP, Pusavec F, Zacny KA, Taylor LA, Dillon OW Jr, Rouch K, Jawahir IS (2008) Modeling and optimization of PCD compact core drilling of basalt rock, CIRP-ICME'08. Naples, Italy
- Hamade RF, Manthri SP, Pusavec F, Zacny KA, Taylor LA, Dillon Jr. OW, Rouch K, Jawahir IS (2009) Developing a methodology towards sustainable PCD compact core drilling on planet Mars, IMECE2009-10133. In: Proceedings of the ASME international mechanical engineering congress and exposition, Lake Buena Vista, FL, USA.
- Hamade RF, Manthri SP, Pusavec F, Zacny KA, Taylor LA, Dillon OW Jr, Rouch K, Jawahir IS (2010) Compact core drilling in basalt rock using PCD tool inserts: wear characteristics and cutting forces. *J Mater Process Technol* 210:1326–1339
- Bourgoyne AT, Young FS Jr (1974) A multiple regression approach to optimal drilling and abnormal pressure detection. Paper SPE 4238, Trans, AIME, Soc Pet Eng J 257:371–384
- Judzis A, Bland RG, Curry DA, Black AD, Robertson HA, Meiners MJ, Grant TC (2009) Optimization of deep-drilling performance—benchmark testing drives ROP improvements for bits and drilling fluids. *SPE Drill Complet* 24(1):25–39
- Venet V, Henry JP, Fourmaintraux D (1993) Contribution to the optimizing of core drilling by modeling the initiation of discing. *Revue de L Institut Francais Du Petrole* 48(1):15–42
- Yinghui L, Mavroidis C, Bar-Cohen Y, Zensheu C (2007) Analytical and experimental study of determining the optimal number of wedge shape cutting teeth in coring bits used in percussive drilling. *J Manuf Sci Eng (Trans ASME)* 129(4):760–769
- Holland JH (1992) Adaptation in natural and artificial systems. University of Michigan Press, Michigan
- Malakooti B, Deviprasad J (1989) An interactive multiple criteria approach for parameter selection in metal cutting. *Oper Res* 37(5):805–818
- Ali-Tavoli M, Nariman-Zadeh N, Khakhali A, Mehran M (2006) Multi-objective optimization of abrasive flow machining processes using polynomial neural networks and genetic algorithms. *Mach Sci Technol* 10(4):491–510
- Sardiñas RQ, Santana MR, Alfonso E, Brindis EA (2006) Genetic algorithm-based multi-objective optimization of cutting parameters in turning processes. *Eng Appl Artif Intel* 19:127–133
- Zhang J-Y, Liang SY, Yao J, Chen JM, Huang JL (2006) Evolutionary optimization of machining processes. *J Intell Manuf* 17(2):203–215
- Wang X, Jawahir IS (2005) Optimization of multi-pass turning operations using genetic algorithms for the selection of cutting conditions and cutting tools with tool-wear effect. *Int J Prod Res* 43(17):3543–3559
- Clayton R, Chen S, Lefort G (2005) New Bit design, cutter technology extend PDC applications to hard rock drilling. In: SPE/IADC drilling conference proceedings, Amsterdam, the Netherlands, 23–25 February 2005
- Weaver GE et al. (2000) Method and system for predicting performance of a drilling system for a given formation. US Patent 6109368.
- Plinninger RJ, Spaun G, Thuro K (2002) Prediction and classification of tool wear in drill and blast tunneling. In: van Rooy JL and Jermy, CA (eds) Proceedings of 9th congress of the international association for engineering geology and the environment, Durban, South Africa, 16–20 September 2002. ISBN no. 0-620-28559-1. pp 2226–2236.
- Wojtanowicz AK, Kuru E (1993) Mathematical modelling of PDC bit drilling process based on a single cutter mechanics. *J Energy Resour Tech (Trans ASME)* 115(4):247–256
- Choudhury SK, Kishore KK (2000) Tool wear measurement in turning using force ratio. *Int J Mach Tool Manuf* 40:899–909
- Hamade RF, Seif CY, Ismail F (2006) Extracting cutting force coefficients from drilling experiments. *Int J Mach Tool Manuf* 46:387–396
- Plinninger RJ, Thuro K (2004) Wear prediction in hard rock excavation using the CERCHAR Abrasiveness Index (CAI). In: Shubert (ed) EUROCK 2004 and 53rd Geomechanics Colloquium, 2004 VGE.
- Myers RH, Montgomery DC (1995) Response surface methodology: process and product optimization using designed experiments. Wiley, New York (Probability and Statistics Series)